DEUTSCHES ELEKTRONEN – SYNCHROTRON

DESY 93-039
TSL/ISV-93-0081
March 1993

Heavy Majorana Neutrinos at *ep* Colliders

G. Ingelman
Dept. of Radiation Sciences, Uppsala University, Sweden
and
Deutsches Elektronen-Synchrotron DESY, Hamburg

J. Rathsman
Dept. of Radiation Sciences, Uppsala University, Sweden

ISSN 0418-9833

NOTKESTRASSE 85 · D-2000 HAMBURG 52

DESY 93-039
TSL/ISV-93-0081
March 1993

ISSN 0418-9833

Heavy Majorana Neutrinos at *ep* Colliders

G. Ingelman[a,b] and J. Rathsman[a]

[a] Dept. of Radiation Sciences, Uppsala University, Box 535, S-751 21 Uppsala, Sweden
[b] Deutsches Elektronen-Synchrotron DESY, Notkestrasse 85, D-2000 Hamburg 52 FRG

Abstract: Heavy Majorana neutrinos (N), predicted in various extensions of the standard model, are examined with respect to the present limits on their masses and mixings with ordinary leptons resulting in explicit examples of allowed values of interest for present and planned accelerator energies. The decay $N \to Z\nu$ is added to the previously available formalism and all dominating branching ratios are calculated. The production of Majorana neutrinos through charged current interactions in the *ep* colliders HERA and LEP⊕LHC is investigated using Monte Carlo event simulation. Signals in terms of isolated leptons and jets are found and shown to be effective in suppressing the dominating standard model backgrounds. The discovery limits of such Majorana neutrinos are, for a mixing of 1%, about 160 GeV at HERA and 700 GeV at LEP⊕LHC.

1 Introduction

The standard model of electroweak and strong interactions has been remarkably successful in describing the experimental data. Nevertheless, it cannot be the ultimate theory due to its theoretical shortcomings, e.g. for the understanding of the mass and family structure of quarks and leptons and the many free parameters. Although it is conceivable that the standard model gives a proper description of the fundamental interactions all the way up to a grand unification mass scale of $\sim 10^{15}$ GeV, it is also possible that new interactions and particles enter already at TeV energies. Even within the standard model gauge group $SU(3)_C \otimes SU(2)_L \otimes U(1)_Y$ it is possible to have non-zero neutrino masses and heavy right-handed neutrinos. Attempts to solve the theoretical problems of the standard model have been made based on various theoretical grounds and several extended theories have been suggested and studied in detail. These theories are normally based on some larger symmetry group which unifies the interactions and is spontaneously broken down to the standard model gauge group. Particular attention has been given to models with an additional $U(1)$ symmetry or with left-right symmetry in the form $SU(2)_L \otimes SU(2)_R \otimes U(1)_{B-L}$, which can both be subgroups of the unification groups $SO(10)$ and E_6. The questions of neutrino masses and lepton number violation, which are of general importance (for a review see [1]), enter explicitly in this context and, in particular, heavy Majorana neutrinos may be present [2].

As an explicit example one may consider gauge theories based on the unification group $SO(10)$ where only one additional fermion, namely a right-handed neutrino ν_R, is required for each quark-lepton generation. The group $SO(10)$ contains a $U(1)_{Y'}$ symmetry in addition to the standard model hypercharge and thereby also an additional gauge boson Z'. The spontaneous breaking of this extra symmetry generates neutrino masses in proportion to the Z' mass [3]. Consequently, with the existence of a Z' with mass of order 1 TeV follows naturally neutrinos with masses in the range tens of GeV to hundreds of GeV. The Majorana nature of these neutrinos is related to the violation of lepton number (or difference between baryon and lepton number $B - L$) that arises in these theories. The production of such Majorana neutrinos can occur by the normal standard model interactions, but are then suppressed by their small mixing with the ordinary leptons [2].

Another class of models is based on the symmetry group $SU(2)_L \otimes SU(2)_R \otimes U(1)_{B-L}$ with right-handed weak currents and massive right-handed neutrinos. Majorana neutrinos can here be produced without mixing, but are instead suppressed by the large mass of the right-handed boson W_R [4]. The present bound on this mass is $m_{W_R} > 450$ GeV [4] and leads to less promising discovery limits compared to the previous case with mixing [2, 4]. We will therefore in the following concentrate on the first class of models and only work out detailed search strategies for them. This is further motivated through the relative simplicity of this mixing scenario which, for our purposes, can be seen as a more general example representative for various theories independent of their details. The left-right symmetry case requires the introduction of more details concerning masses and couplings of new currents and is therefore somewhat more model dependent.

The paper is organised as follows. In section 2 we present the formalism for production and decay of heavy Majorana neutrinos through mixing in ordinary weak interactions. Section 3 concerns present limits on masses and mixings and we explicitly demonstrate the possibility of values such that the production cross-sections at present and future *ep* colliders are of experimental interest. The detailed investigation of signatures for a Majorana neutrino search and the standard model backgrounds are investigated in section 4. Finally, we summarise and conclude in section 5.

2 Production and decay through mixing

The simplest process, in terms of minimal new physics assumptions, to produce heavy Majorana neutrinos in *ep* collisions is through normal charged current interactions as illustrated in Fig. 1. The cross-section is suppressed, not only by limited phase space due to the large neutrino mass m_N, but also by the required mixing ξ between light and heavy Majorana neutrinos [6, 2, 5]. The light Majorana neutrinos can be identified with the normal neutrinos ν_e, ν_μ and ν_τ, whose small masses is naturally explained through the see-saw mechanism [1]. The mixing in the leptonic part of the charged current interaction is given by a unitary Kobayashi-Maskawa type matrix V and the matrix ξ. A power series in ξ gives the connection between the weak eigenstates ν_L, ν_R and the Majorana mass eigenstates ν, N [6], *i.e.* $\nu_L = \frac{1-\gamma_5}{2}(\nu + \xi N + ...)$, $\nu_R = \frac{1+\gamma_5}{2}(N - \xi^T \nu + ...)$.

The heavy Majorana neutrinos will decay into either $\nu_\ell Z^0$, $\ell^+ W^-$ or $\ell^- W^+$ where the weak bosons can be taken as being on-shell since we only consider Majorana neutrino masses above the boson masses ($m_N > m_B$) due to mass limits discussed in section 3.

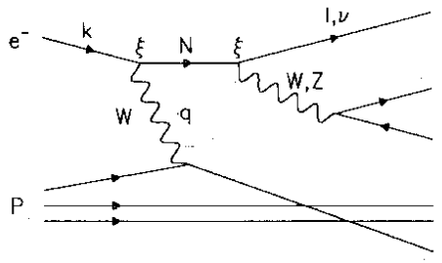

Figure 1: *Production (in ep collisions) and decays of heavy Majorana neutrinos.*

Using the narrow width approximation for the heavy Majorana neutrino propagator in Fig. 1, the cross-section for the process $e^- p \to NX$ where $N \to \ell^\pm W^\mp$ or $N \to \nu_\ell Z^0$ is [2]

$$\begin{aligned}\frac{d\sigma}{dx\,dy\,dp_{\ell\perp}\,dy_\ell} &= \frac{G_F^3 m_W^6 |(V\xi)_{eN}|^2}{32\sqrt{2}\pi^3 \hat{s} m_N \Gamma_N} \frac{1}{(y\hat{s}+m_W^2)^2} \frac{1}{m_{N\perp}} \\ &\times \left[\cosh(y_N - y_\ell) - \frac{m_N^2 - m_B^2 - 2p_{\ell\perp}p_{N\perp}}{2m_{N\perp}p_{\ell\perp}}\right]^{-1/2} \\ &\times \left[\frac{m_N^2 - m_B^2 + 2p_{\ell\perp}p_{N\perp}}{2m_{N\perp}p_{\ell\perp}} - \cosh(y_N - y_\ell)\right]^{-1/2} \\ &\times \left[A\cdot(u(x,\mu^2)+c(x,\mu^2)) + B\cdot(\bar{d}(x,\mu^2)+\bar{s}(x,\mu^2))\right] \qquad (1)\end{aligned}$$

The independent variables are here chosen as the normal deep inelastic scaling variables x and y together with the transverse momentum $p_{\ell\perp}$ and rapidity y_ℓ of the final state lepton ℓ from the Majorana neutrino decay. With four-momenta as in Fig. 1, $s = (P+k)^2$, $Q^2 = -q^2$ and $\hat{s} = xs$. As usual, $x = Q^2/2P\cdot q$ and $y = P\cdot q/P\cdot k$, but they are kinematically constrained to

$$\frac{m_N^2}{s} \le x \le 1 \quad , \quad 0 \le y \le 1 - \frac{m_N^2}{\hat{s}} \quad . \qquad (2)$$

The indices N and W denote the Majorana neutrino and the W boson exchanged in the t-channel, whereas B and ℓ denote the weak boson and lepton from the Majorana neutrino decay, respectively. The symbols y_ℓ, y_N, m, $m_\perp = \sqrt{m^2+p_\perp^2}$ and $p_\perp$ refer to rapidity, mass, transverse mass and transverse momentum, respectively. All frame dependent quantities are understood to be in the lab frame. Γ_N is the total width of the Majorana neutrino and the functions u, c, $\bar{d}$ and $\bar{s}$ are the parton density functions in the proton evaluated at a suitable scale μ.

The coefficient functions A, B depend on the decay products of the Majorana neutrino as follows [2]

$$\begin{aligned}A(\ell^- W^+) &= |(V\xi)_{eN}|^2 \frac{4\hat{s}}{m_W^2} \\ &\left[(m_N^2 - m_W^2)(2m_W^2\hat{s} - m_N^4) - 2m_N^2(2m_W^2 - m_N^2)p_{\ell\perp}(xE_p e^{-y_\ell} + E_e e^{y_\ell})\right] \qquad (3) \\ B(\ell^- W^+) &= |(V\xi)_{eN}|^2 \frac{8(\hat{s}(1-y) - m_N^2)}{m_W^2}\end{aligned}$$

$$\left[\hat{s}(1-y)m_W^2(m_N^2 - m_W^2) - m_N^2(2m_W^2 - m_N^2)p_{\ell\perp}xE_p e^{-y_\ell}\right] \qquad (4)$$

$$\begin{aligned}A(\ell^+ W^-) &= |(V\xi)_{eN}|^2 \frac{4\hat{s}m_N^2}{m_W^2} \\ &\left[(m_N^2 - m_W^2)(\hat{s} - 2m_W^2) + 2(2m_W^2 - m_N^2)p_{\ell\perp}(xE_p e^{-y_\ell} + E_e e^{y_\ell})\right] \qquad (5) \\ B(\ell^+ W^-) &= |(V\xi)_{eN}|^2 \frac{4m_N^2(\hat{s}(1-y) - m_N^2)}{m_W^2} \\ &\left[\hat{s}(1-y)(m_N^2 - m_W^2) + 2(2m_W^2 - m_N^2)p_{\ell\perp}xE_p e^{-y_\ell}\right] \qquad (6)\end{aligned}$$

To complete this cross-section formalism we have also calculated the matrix elements for the neutral current decay $N \to \nu_\ell Z$ resulting in

$$A(\nu_\ell Z) = |\xi_{\nu_\ell N}|^2 \frac{2\hat{s}(\hat{s} - m_N^2)(m_N^2 - m_Z^2)(m_N^2 + 2m_Z^2)}{\cos^2\theta_W m_Z^2} \qquad (7)$$

$$B(\nu_\ell Z) = |\xi_{\nu_\ell N}|^2 \frac{2\hat{s}(1-y)(\hat{s}(1-y) - m_N^2)(m_N^2 - m_Z^2)(m_N^2 + 2m_Z^2)}{\cos^2\theta_W m_Z^2} \qquad (8)$$

The total width of the heavy Majorana neutrino is given by

$$\begin{aligned}\Gamma_N &= \sum_\ell \frac{G_F}{8\sqrt{2}\pi m_N^3}\left[2|(V\xi)_{\ell N}|^2(m_N^2 - m_W^2)^2(m_N^2 + 2m_W^2)\right. \\ &\left. + |\xi_{\nu_\ell N}|^2(m_N^2 - m_Z^2)^2(m_N^2 + 2m_Z^2)\right] \qquad (9)\end{aligned}$$

and the partial widths are

$$\Gamma(N \to \ell^\pm W^\mp) = \frac{|(V\xi)_{\ell N}|^2}{8\sqrt{2}\pi}\frac{G_F}{m_N^3}(m_N^2 + 2m_W^2)(m_N^2 - m_W^2)^2 \qquad (10)$$

$$\Gamma(N \to \nu_\ell Z) = \frac{|\xi_{\nu_\ell N}|^2}{8\sqrt{2}\pi}\frac{G_F}{m_N^3}(m_N^2 + 2m_Z^2)(m_N^2 - m_Z^2)^2 \qquad (11)$$

Assuming the Kobayashi-Maskawa type matrix V for the lepton sector to be diagonal, so that $|(V\xi)_{\ell N}| = |\xi_{\nu_\ell N}|$, we obtain the branching ratios shown in Fig. 2. Although all

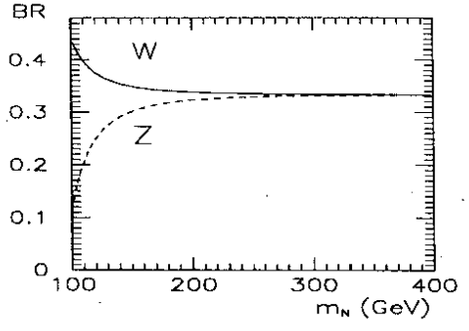

Figure 2: *Branching ratios for $N \to \ell^\pm W^\mp$ (full curve) and $N \to \nu_\ell Z^0$ (dashed curve) as a function of the Majorana neutrino mass m_N.*

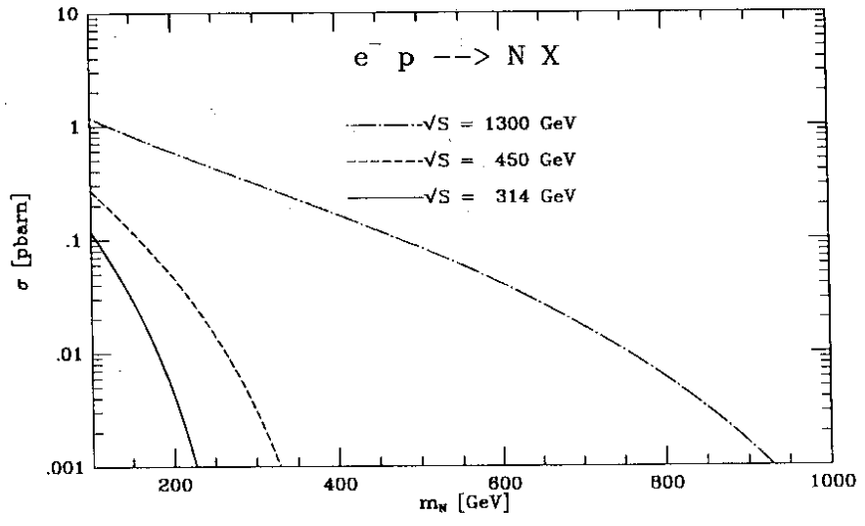

Figure 3: *Total cross section for $ep \to NX$, via W exchange, assuming the mixing $|(V\xi)_{eN}|^2 = 0.01$, at three center-of-mass energies corresponding to HERA, a HERA upgrade and LEP⊕LHC. From [2].*

	E_e [GeV]	E_p [GeV]	$\sqrt{s}$ [GeV]	$\int_{\sim 1\,year} dt\,\mathcal{L}$ [pb^{-1}]	max m_N [GeV]
HERA	30	820	314	200	160
HERA upgrade	45	1140	450	1000	280
LEP⊕LHC	50	8000	1265	1000	820

Table 1: *ep colliders and their Majorana neutrino discovery potential.*

three are 1/3 at large Majorana neutrino masses, for masses not far above the W and Z masses there is a substantial phase space suppression of the decay into the Z.

The magnitude of the total cross-section for the production of a Majorana neutrino as a function of its mass is shown in Fig. 3 for the *ep* collider configurations specified in Table 1. In this numerical example [2], the Duke-Owens parton densities [7] are used and the mixing $|(V\xi)_{eN}|^2 = 0.01$ assumed. With the integrated luminosities in Table 1 and the requirement of at least, say, 5 events the Majorana neutrino mass limits in Table 1 are obtained as a crude estimate of the discovery potential. In section 4 this will be studied in more detail based on Monte Carlo simulations.

3 Present limits on masses and mixings

In this section we demonstrate that the present limits of relevance for heavy Majorana neutrinos do not exclude their existence with parameters such that they can be produced at present and future *ep* colliders. The possible masses (m_N) and mixings ($\xi_{\nu_\ell N}$) of

Majorana neutrinos are constrained by several kinds of experimental information. These include both direct searches for Majorana neutrino production and indirect methods where such neutrinos can be involved in the process such as neutrinoless double β-decay, charged current universality, Γ_{inv} at the LEP-experiments. In addition, solar neutrinos and dark matter have implications on heavy neutrinos, but such limits are weaker and more model dependent. For reviews on the physics of massive neutrinos see ref. [1].

In e^+e^- annihilation at LEP, direct searches for neutral heavy leptons have been made (see e.g. [8, 9]) with the most stringent limit being [9]

$$Br(Z \to \nu_\ell N_\ell) < 3 \times 10^{-5} \quad \text{at 95\% CL for} \quad 3\,GeV < m_N < m_Z \tag{12}$$

From the branching ratio formula

$$Br(Z \to \nu_\ell N_\ell) = Br(Z \to \nu_\ell \bar{\nu}_\ell)|\xi_{\ell\ell}|^2 (1 - \frac{m_N^2}{m_Z^2})^2 (1 + \frac{1}{2}\frac{m_N^2}{m_Z^2}) \tag{13}$$

one can conclude that $m_N > 82$ GeV for $|\xi_{e1}|^2 = 0.01$.

To elaborate on the limits obtained indirectly from various processes one must consider the Majorana neutrino formalism in some more detail. In the notation used (cf. [2]) the neutrino mass matrix is given by $\mathcal{M} = \begin{pmatrix} 0 & m_D \\ m_D^T & M \end{pmatrix}$ where the Majorana mass matrix M can be chosen real and diagonal, but the Dirac mass matrix m_D is then, in the most general case, complex

$$M = \begin{pmatrix} M_1 & 0 & 0 \\ 0 & M_2 & 0 \\ 0 & 0 & M_3 \end{pmatrix} \quad , \quad m_D = \begin{pmatrix} m_{11} & m_{12} & m_{13} \\ m_{21} & m_{22} & m_{23} \\ m_{31} & m_{32} & m_{33} \end{pmatrix}$$

Diagonalising the total mass-matrix to first order in $\xi = m_D \frac{1}{M}$ (assuming $m_D \ll M$) gives the masses of the mass eigenstates ν_ℓ and N_ℓ of the light and heavy neutrinos, respectively,

$$\begin{pmatrix} m_\nu & 0 \\ 0 & m_N \end{pmatrix} = \begin{pmatrix} -m_D \frac{1}{M} m_D^T & 0 \\ 0 & M \end{pmatrix}$$

Following the appendix in [2] we write the Dirac mass matrix as $m_D = m_D^{(0)} + \epsilon\, m_D^{(1)}$. The experimental upper mass limits [10] on the normal neutrinos ν_e, ν_μ, ν_τ can be satisfied by requiring the light neutrinos to be massless to zeroth order in the seesaw formula, *i.e.* $m_\nu^{(0)} = -m_D^{(0)} \frac{1}{M} m_D^{(0)T} = 0$. This gives the general solution

$$m_D^{(0)} = \begin{pmatrix} m_1 & m_2 & m_3 \\ \alpha m_1 & \alpha m_2 & \alpha m_3 \\ \beta m_1 & \beta m_2 & \beta m_3 \end{pmatrix}$$

where

$$\frac{m_1^2}{M_1} + \frac{m_2^2}{M_2} + \frac{m_3^2}{M_3} = 0 \tag{14}$$

must be fulfilled to get $m_\nu^{(0)} = 0$. (This is a stronger constraint on the parameters than in [2], but those authors agree with our result.) Requiring m_ν to be diagonal and not identically vanishing to order ϵ gives the requirement $\alpha\beta = 0$. Choosing $\beta = 0$ then gives that the mixing matrix ξ is given by

$$\xi = \begin{pmatrix} \frac{m_1}{M_1} & \frac{m_2}{M_2} & \frac{m_3}{M_3} \\ \alpha\frac{m_1}{M_1} & \alpha\frac{m_2}{M_2} & \alpha\frac{m_3}{M_3} \\ 0 & 0 & 0 \end{pmatrix} + \mathcal{O}(\epsilon) \ .$$

From neutrinoless double β-decay, where a Majorana neutrino can be exchanged in the t-channel, one can derive the two limits [11]

$$\sum_{i=e}^{\tau}(V)_{ei}^2 m_{\nu_i} \;<\; 1\,eV \tag{15}$$

$$\sum_{i=1}^{3}(V\xi)_{ei}^2\frac{1}{M_i} \;\lesssim\; 10^{-7}GeV^{-1} \tag{16}$$

The second limit is uncertain due to the poor knowledge of the wavefunctions of the nucleons and may, depending on the model used, vary with an order of magnitude [12]. The first limit is automatically fulfilled if ϵ is small since, as discussed, the light neutrinos are massless to zeroth order in ϵ if eq. (14) holds.

We will now show that it is possible to have a Majorana neutrino mass as low as $\sim$ 100 GeV and still a mixing as large as $\sim$ 1%, even if we set the condition given by eq. (16) to zero. Together with eq. (14) we thus get two conditions that have to be fulfilled. To study these conditions in more detail we introduce the following variables,

$$a = \frac{m_1^2}{M_1}\exp i\phi \qquad b = \frac{m_2^2}{M_2}\exp i\phi \qquad c = \frac{m_3^2}{M_3}\exp i\phi \tag{17}$$

where ϕ is chosen such that a is real and positive. The two conditions, (14) and (16), can then be expressed in the following way

$$\begin{aligned} a+b+c &= 0 \\ \frac{a}{M_1^2}+\frac{b}{M_2^2}+\frac{c}{M_3^2} &= 0 \end{aligned} \tag{18}$$

where $V = 1$ has been chosen for simplicity. Solving for b and c gives

$$b \;=\; a\frac{M_2^2}{M_1^2}\frac{M_1^2-M_3^2}{M_3^2-M_2^2} \tag{19}$$

$$c \;=\; a\frac{M_3^2}{M_1^2}\frac{M_1^2-M_2^2}{M_2^2-M_3^2} \tag{20}$$

and we note that b and c are also real. With b and c being fixed from (19) and (20) we can still choose a, M_1, M_2, M_3 to fulfill the requirements from charged current universality and lepton universality in π-decays given by [13, 14]

$$|\xi_{e1}|^2 + |\xi_{e2}|^2 + |\xi_{e3}|^2 < 0.01 \tag{21}$$

which translates into

$$\frac{|a|}{|M_1|}+\frac{|b|}{|M_2|}+\frac{|c|}{|M_3|} < 0.01 \tag{22}$$

A numerical example which complies with this limit is given by, $a = 0.5$ GeV, $M_1 = 100$ GeV, $M_2 = 150$ GeV and $M_3 = 1000$ GeV giving $b = -1.14$ GeV and $c = 0.64$ GeV. From eq. (17) we then get $m_1 = 7.1$ GeV, $m_2 = 13.1i$ GeV and $m_3 = 25.3$ GeV which gives $|\xi_{e1}|^2 = 0.0050$, $|\xi_{e2}|^2 = 0.0076$ and $|\xi_{e3}|^2 = 0.0006$. Finally, adding gives $|\xi_{e1}|^2 + |\xi_{e2}|^2 + |\xi_{e3}|^2 = 0.013$ which is in agreement with the 1σ-limit in eq. (21).

We also get a relation between the mixings ξ_{ei} which says that the lightest of the heavy Majorana neutrinos cannot have the largest mixing. It follows from rewriting the solutions for b and c, eqs. (19) and (20), in the following way:

$$|\xi_{e2}|^2 \;=\; |\xi_{e1}|^2\frac{|M_2|}{|M_1|}\frac{M_3^2-M_1^2}{M_3^2-M_2^2} \tag{23}$$

$$|\xi_{e3}|^2 \;=\; |\xi_{e1}|^2\frac{|M_3|}{|M_1|}\frac{M_2^2-M_1^2}{M_3^2-M_2^2} \tag{24}$$

where we have assumed $|M_1| < |M_2| < |M_3|$. If we require that $|\xi_{e1}|^2$ is the largest mixing, *i.e.* $|\xi_{e2}|^2 < |\xi_{e1}|^2$ and $|\xi_{e3}|^2 < |\xi_{e1}|^2$ then eqs. (23) and (24) gives $|M_2| < |M_1|$. This contradicts our assumption that $|M_1| < |M_2|$ and we therefore conclude that $|\xi_{e1}|^2 < |\xi_{e2}|^2$ if $|M_1| < |M_2|$.

From our explicit example we see the possibility to have a Majorana neutrino mass as low as $\sim$ 100 GeV and still a mixing as large as $\sim$ 1%. As shown in section 2, this leads to production cross-sections that are large enough to be of experimental interest. In the following we develop search strategies which should either lead to their discovery or more stringent bounds on their mass and mixing parameter.

4 Search strategies at *ep* colliders

In order to study in more detail the physics of heavy Majorana neutrinos in *ep* collisions we have used Monte Carlo methods to simulate complete events. As motivated above, we only consider the production of Majorana neutrinos through exchange of normal W bosons. For their mixing with light neutrinos we have assumed the value $|(V\xi)_{eN}|^2 = |\xi_{\nu_e N}|^2 = 0.01$ and for their masses values of 100 GeV or higher, both in accordance with the limits in section 3. Since the mixing parameter is an overall factor, our results can easily be rescaled to any other value. We compare the prospects at the HERA collider and a possible future *ep* collider based on the electron beam in LEP and the proton beam in LHC. The energies and typical integrated luminosities used are the design values as specified in Table 1. Under these conditions the cross-section as a function of the Majorana neutrino mass is given in Fig. 3. It is, for example 103 fb for $m_N = 100$ GeV at HERA and 86 fb for $m_N = 500$ GeV at LEP⊕LHC. These masses are taken as representative cases for the detailed results below, although final results are also given for the masses m_N=100, 300 and 700 GeV at LEP⊕LHC and m_N=160 GeV at HERA. The Majorana neutrino search strategies are worked out taking also the most important background processes into account.

4.1 Monte Carlo event generator

We have constructed a dedicated Monte Carlo program, MAJOR 1.2, which is an upgraded version of [15]. The program simulates complete events where heavy Majorana neutrinos are produced and decayed. The importance sampling method is used to generate phase space points according to the differential cross section formula in eq. (1) (for details, see [16]). For the proton structure functions we take parameterisation 1 of EHLQ [17] using Q^2 as scale. From the phase space point $(x, y, p_{\ell\perp}, y_\ell)$, the four-momenta of all particles

(partons) in the Feynman diagram of Fig. 1 are calculated. The Lund Monte Carlo programs LEPTO 6.1 [18] and JETSET 7.3 [19] are then used to produce a complete final state of observable particles. The on-shell W/Z (from the heavy neutrino decay) is decayed with the proper branching ratios into a lepton pair or a $q\bar{q}'$ pair, where the polarisation of the W/Z is not taken into account. In the latter decay mode of the W/Z boson, parton showers are included to account for QCD radiation of additional partons, and this parton system is then hadronised using the Lund string model [20, 19]. Similarly, the quark entering and leaving the deep inelastic scattering may radiate partons through initial and final state parton showers. Together with the proton remnant spectator, this parton system is hadronised with the Lund model. Thus, the complete 'history' of the event is generated resulting in a complete final state.

4.2 Characteristics of Majorana neutrino events

The energy threshold to produce a heavy neutrino implies the limits for x and y given in eq. (2), in particular small values of x are excluded. The large x-values imply that the scattering is mainly on valence u-quarks in the proton and that there is not much initial state gluon radiation.

It is assumed that the heavy Majorana neutrino produced is the lightest one and belongs to the first generation. The Majorana neutrino can then decay into $\nu_\ell Z$, ℓ^+W^- or ℓ^-W^+ where ℓ is any charged lepton, but here we will simplify by assuming no mixing between lepton families ($(V\xi)_{\mu 1} = (V\xi)_{\tau 1} = 0$), *i.e.* we only consider the decay modes e^+W^-, e^-W^+ and $\nu_e Z$, with branching ratios given by eqs. (10,11) and shown numerically in Fig. 2. The channel $N \to e^+W^-$ should be noted in particular since it implies lepton number violation. If there is mixing between the families, decays into τ leptons may be harder to reconstruct experimentally, whereas decays into muons would provide two channels ($\mu^\pm$) that should be easier to detect and have less background than the $e^\pm$ signal studied below.

The distribution of the rapidity and transverse momentum (in the lab frame) of the positron from the N-decay is shown in Fig. 4. The rapidities are reasonably central, even at LEP⊕LHC with its very strong boost of the ep system along the proton beam direction, and therefore mostly within the detector acceptance region. The distribution of the electrons is almost identical but for the neutrinos there is a shift to lower $p_\perp$ due to the larger Z-mass. The transverse momentum of the lepton from the neutrino decay depends strongly on the difference between the Majorana neutrino mass and the W/Z mass as can be seen from comparing Figs. 4c and d. It is in any case quite large, which favours its detection.

The W/Z-boson from the N decay will either decay into a quark-antiquark pair giving two jets or into a lepton pair. These decay products will also have quite large transverse momenta and mostly be in a detectable rapidity region. The $q\bar{q}'$ pair from the W/Z decay will produce two jets with invariant mass $m_{W/Z}$, which provides another characteristic feature. Taking all neutrino decay products into account, it is natural to investigate the following four signals for the Majorana neutrino:

1. a high-$p_\perp$ isolated **positron** and two jets with $m_{ij} \simeq m_W$
2. a high-$p_\perp$ isolated **electron** and two jets with $m_{ij} \simeq m_W$

3. a high-$p_\perp$ **neutrino** giving a large missing $p_\perp$ and two jets with $m_{ij} \simeq m_Z$
4. two high-$p_\perp$ isolated leptons with opposite charges

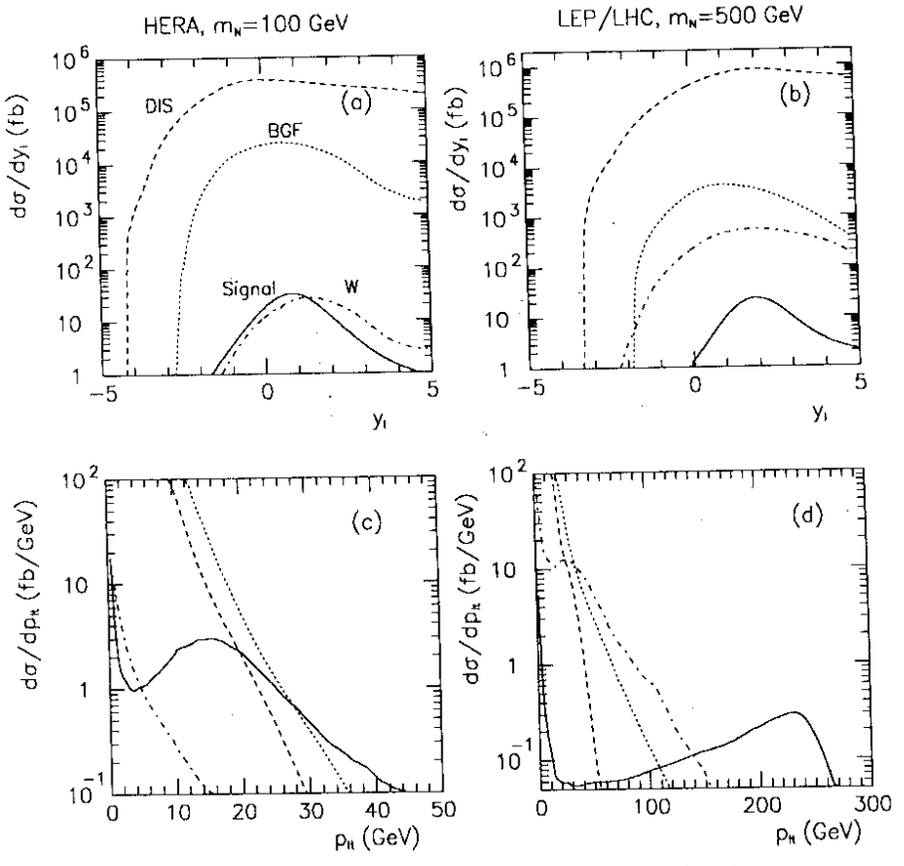

Figure 4: *The differential cross-sections for laboratory rapidity (a,b) and transverse momentum (c,d) of positrons from the Majorana neutrino decay (full curves) and the backgrounds due to DIS (dashed curves), heavy flavour production (dotted curves) and W production (dash-dotted curves). (a,c) HERA conditions ($\sqrt{s} = 314\ GeV$) with Majorana neutrino mass $m_N = 100\ GeV$; (b,d) LEP⊕LHC conditions ($\sqrt{s} = 1.3\ TeV$) with $m_N = 500\ GeV$.*

4.3 Background processes

The dominating standard model background processes are normal deep inelastic scattering (DIS), boson-gluon fusion (BGF) into heavy quarks and W production, as illustrated in

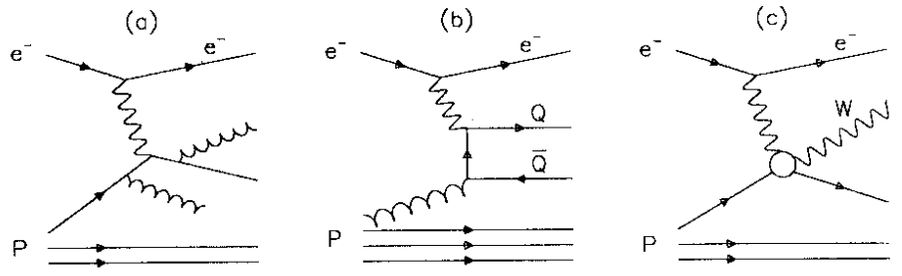

Figure 5: *The dominating background processes: (a) deep inelastic scattering, (b) heavy flavour production and (c) W production.*

Fig. 5. We have made complete event simulation of these processes to facilitate a detailed comparison with the Majorana neutrino event characteristics. In DIS the scattered lepton provides an isolated electron or neutrino signature and a jet pair may arise through QCD parton radiation as illustrated in Fig. 5a. Such events are simulated using the Monte Carlo LEPTO 6.1 [18] based on the electroweak cross-sections and first order QCD matrix elements plus parton showers for the higher order parton emission processes.

Isolated leptons may also arise in the decay of heavy quarks and we therefore simulate boson-gluon fusion into $b\bar{b}$, $b\bar{t}$ and $t\bar{t}$ pairs using the Monte Carlo AROMA 1.4 [21] assuming that $m_t = 150\,GeV$. (The production of $c\bar{c}$ was included in the simulation with LEPTO 6.1, but the energy release in c-quark decay is to small to give an important contribution to isolated high $p_\perp$ leptons.) It is not possible to produce t-quarks at HERA, but at LEP⊕LHC it is important to include them, since, although the cross-section is very small, it gives the dominating contribution to the BGF background. Jets may in the BGF process arise from the produced heavy quarks themselves and the additional parton emission simulated by parton showers.

The production of on-shell W bosons will in their decay give either two jets or two leptons just as the W bosons from the heavy Majorana neutrino decays. An on-shell W can be produced in several ways, e.g. radiated from a quark (Fig. 5c) or a lepton or produced in a triple boson vertex (*cf.* [22]). An isolated lepton can here either be the scattered lepton, but this requires a large Q^2 which lowers the cross-section, or it can come from a leptonic W decay, but then there should be no jet pair giving the W mass. To investigate this process in detail, we use the Monte Carlo generator EPEWAX 1.2 [23] which also provides a complete hadronic final state.

4.4 Signal-to-background

The rate of background events is overwhelming as illustrated by Fig. 4 for the positron signal case. Although a cut in $p_\perp$ of the positron reduces the background by many orders of magnitude, it is not enough unless the Majorana mass is very large so that a sufficiently high $p_\perp$-cut can be chosen without loss of the signal. To start a selection procedure for Majorana neutrino events it is natural to require a high-$p_\perp$ lepton in a selected, observable

rapidity region where its cross-section is maximal. Thus, the cuts used for the first lepton in the two-lepton signal, and for the signal with a positron/electron plus two jets can preferably be chosen as $p_{\ell\perp} > 10$ GeV and $-1 < y_\ell < 3$ for $m_N = 100$ GeV at HERA and $p_{\ell\perp} > 100$ GeV and $0 < y_\ell < 3$ for m_N=500 GeV at LEP⊕LHC. For the signal with a neutrino and two jets we use instead a cut in missing transverse momentum $\not{p}_\perp > 10$ GeV at HERA and $\not{p}_\perp > 100$ GeV at LEP⊕LHC. The $\not{p}_\perp$ is calculated from the observable particles within $5° < \theta < 175°$ and here we also reject events with an isolated high $p_\perp$ charged lepton in the same detector region.

An expected characteristic of leptons from both the N and W/Z decays is that they should be isolated in phase space which is also necessary for a safe e^+/e^--identification. To investigate the isolation we consider the 'accompanying' energy, E_{acc}, within a cone around the lepton. This cone is here defined by $\Delta R \equiv \sqrt{(\Delta\eta)^2 + (\Delta\phi)^2}$, where $\Delta\eta$ and and $\Delta\phi$ are the distances in laboratory pseudorapidity and azimuthal angle (around the beam axis) from the lepton momentum direction. A lepton is then considered isolated if the summed energy of all particles in the cone is less than some maximum allowed energy, E_{acc}. Fig. 6 shows the total cross-section as a function of this allowed accompanying energy to the positron with highest $p_\perp$ in the event. The isolation of the positrons from the Majorana neutrino decay as compared to the background positrons is here clearly demonstrated. In fact, it is so well isolated that a rather large cone can be used together with a very restrictive energy cut, without a significant loss in cross section. For the following analysis we have chosen $\Delta R = 0.5$ and $E_{acc} < 1$ GeV for the positron with highest $p_\perp$. One should note, however, that this isolation requirement has not enough effect when applied to electrons, since isolated high-$p_\perp$ electrons appear with much larger cross-section through the normal neutral current DIS process.

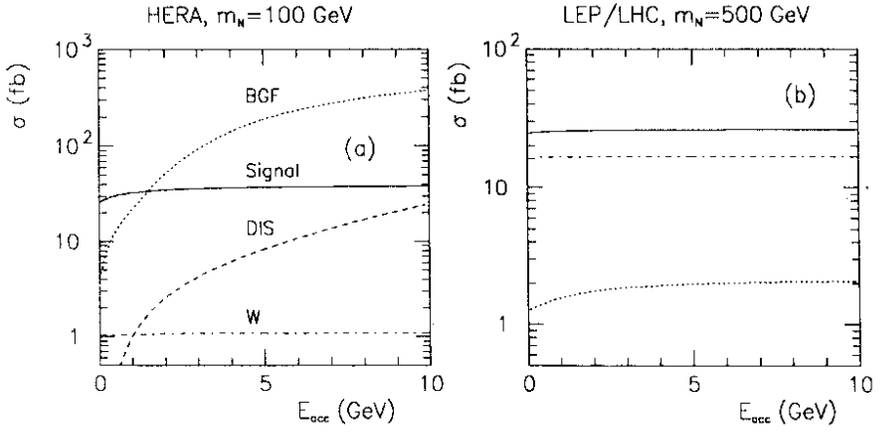

Figure 6: *The cross-section for positrons (with highest $p_\perp$) as a function of their accompanying energy E_{acc} within in a cone $\Delta R \equiv \sqrt{(\Delta\eta)^2 + (\Delta\phi)^2} = 0.5$ obtained from simulated ep collider events at (a) $\sqrt{s} = 314$ GeV and (b) $\sqrt{s} = 1.3$ TeV. The curves correspond to the Majorana neutrino signal (full) and the backgrounds from DIS (dashed), heavy flavours (dotted), W production (dash-dotted).*

The $q\bar{q}$ pair from the W/Z decay will, after QCD gluon radiation and hadronisation, produce a hadronic system with invariant mass $m_{W/Z}$. Unless the parton cascade emission produced extra resolvable jets, there should typically be two jets, which after reconstruction can be required to yield a jet-jet invariant mass, m_{ij}, close to $m_{W/Z}$. We reconstruct the jets with the JADE algorithm in LUCLUS [19]. Here, the pair of particles (or clusters) with the smallest invariant mass are joined together into a cluster. This procedure is repeated for each resulting configuration until all remaining pairs in the event have an invariant mass that exceeds a cut-off, *i.e.* $m_{ij}^2 > y_{cut} M^2$ where M is the invariant mass of the complete hadronic system in the event. The final clusters are then the jets in the event. The parameter y_{cut} can be chosen so as to reconstruct the jets in the signal events as well as possible, *i.e.* ideally four jets including the proton remnant jet (cf. Fig. 1). In addition one should suppress multijet events in background processes which favours a large y_{cut}. After investigations of jet reconstruction on Monte Carlo events we have chosen $y_{cut} = 0.04$ at HERA-energies and $y_{cut} = 0.004$ at LEP⊕LHC-energies as a compromise between these two requirements.

We note that although many particles from the proton remnant jet are lost in the beam pipe, it should be reconstructed to get a proper assignment of particles to jets. In our case we simply include all particles, whereas experimentally one would assign the missing longitudinal momentum in the event to a pseudoparticle which is then included in the jet algorithm leading to a sufficiently good reconstruction of the spectator jet [24]. This jet (identified as the one along the proton beam direction) can then be avoided when the invariant mass of pairs of reconstructed jets are used to find the W or the Z. Therefore, it is not possible to reconstruct the W/Z mass in two-jet events and we add the requirement of at least three jets in the event. With this jet reconstruction procedure one can now investigate signals based on jets.

4.4.1 High-$p_\perp$ lepton and two jets

We first consider the process $e^- p \to NX$ with the lepton number violating decay $N \to e^+ W^-$ and where $W \to q\bar{q}'$ gives jets. Applying the requirements as discussed, and summarised in Table 2, for the positron $p_\perp$, rapidity and isolation as well as on the jets we obtain the jet-jet invariant mass distributions in Fig. 7ab. The mass peak from the W in the signal events is clearly observable and a requirement of a properly reconstructed W-mass within $\pm 5\ GeV$ can be added to select the signal.

The resulting cross-sections for signal and backgrounds after the various cuts are compared in Table 2. The requirement of an isolated high-$p_\perp$ *positron* leaves a small tail of the background surviving the cuts in $p_\perp$ and rapidity. However, when adding the jet requirement, this is reduced to a negligible level. The theoretically available cross section for the signal is in this case at HERA $103\ fb \times 44\% \times 68\% = 31\ fb$ to be compared with the extracted 9 fb, whereas at LEP⊕LHC it is $86\ fb \times 33\% \times 68\% = 19\ fb$ to be compared with the extracted 13 fb. The main loss at LEP⊕LHC is in the reconstruction of the W mass, which may be due to partial overlap (or merging) between the current jet and one of the jets from the W-decay. The production of three resolvable jets due to the parton shower process in the W decay is rare due to the deliberate choice of a rather large y_{cut} in the jet reconstruction, but such cases could be recovered if the invariant mass of three-jet combinations would also be considered. Thus, it may be possible to keep a somewhat larger fraction of the signal events by further improvements of the jet finding

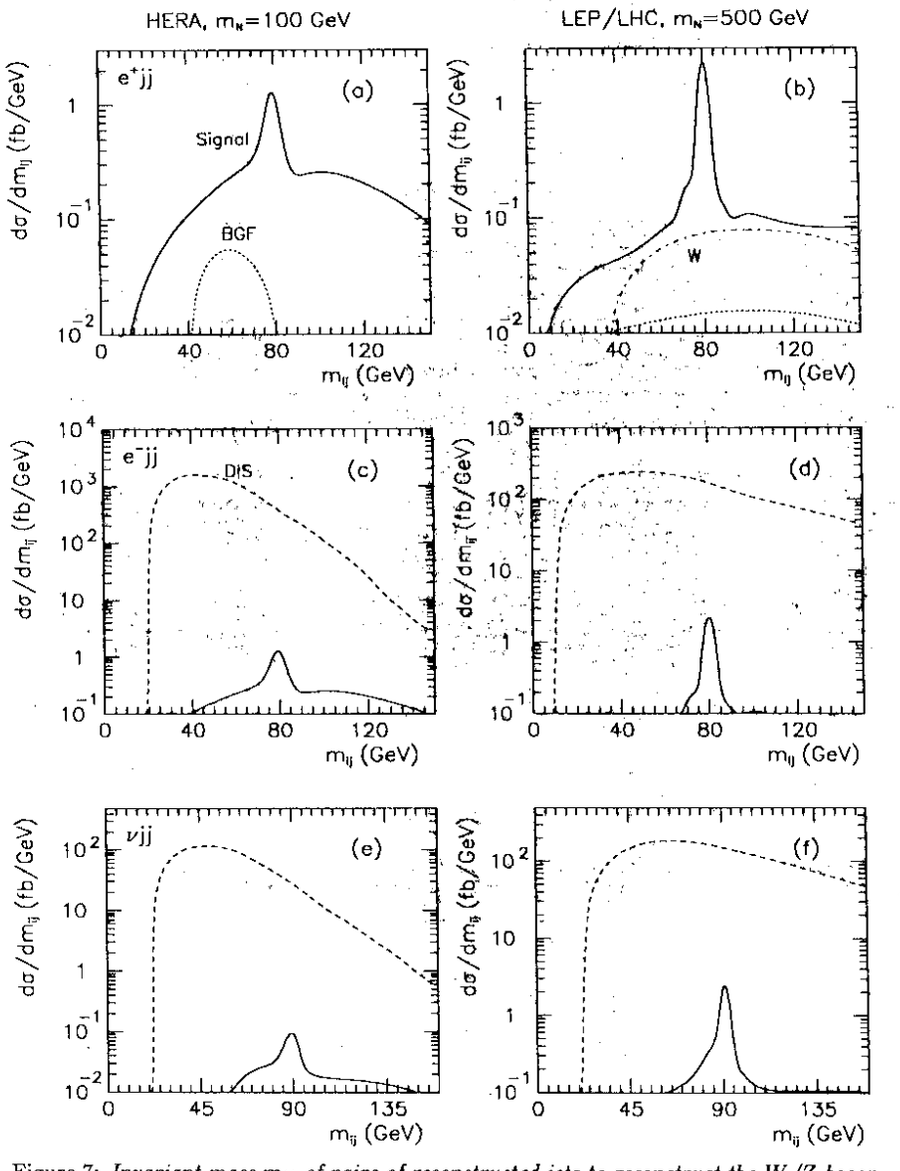

Figure 7: *Invariant mass m_{ij} of pairs of reconstructed jets to reconstruct the W/Z boson. Conditions imposed corresponding to the signals (a,b) isolated high-$p_\perp$ positron and two jets, (c,d) isolated high-$p_\perp$ electron and two jets, (e,f) large $\not{p}_\perp$ and two jets. (a,c,e) HERA ($\sqrt{s} = 314\ GeV$) with Majorana neutrino mass $m_N = 100\ GeV$, (b,d,f) LEP⊕LHC ($\sqrt{s} = 1.3\ TeV$) with $m_N = 500\ GeV$ with curves for the Majorana neutrino signal (full) and the backgrounds from DIS (dashed), heavy flavours (dotted), W production (dash-dotted).*

	Applied cut	Signal	DIS	BGF	W
HERA	Positron: $p_\perp > 10$, $-1 < y_\ell < 3$, $E_{acc} < 1$	32	1.6	20.5	1.0
($m_N = 100$)	Jets: # jets ≥ 3, $75 < m_{ij} < 85$	9.4	0.	0.1	0.1
LEP⊕LHC	Positron: $p_\perp > 100$, $0 < y_\ell < 3$, $E_{acc} < 1$	26	0.	1.6	17
($m_N = 500$)	Jets: # jets ≥ 3, $75 < m_{ij} < 85$	13	0.	0.2	0.9

Table 2: *Cross-sections [fb] for positron and two jets.*

methods, e.g. using the the two step process in [25]. The situation is similar at HERA, where however there are additional losses from the cuts in $p_\perp$ and rapidity (-10%) and the positron isolation requirement (-24%).

From the decay $N \to e^- W^+$ with $W \to q\bar{q}'$ one has the signal of an isolated high-$p_\perp$ *electron* plus two jets, which has a huge background from the normal neutral current DIS. Although the requirement of at least three jets, and in particular a pair of jets with the invariant mass of the W, gives a strong reduction of the cross section it is still much larger than the signal as is shown in Fig. 7cd. There could be some difference in the topology of these signal and background events that may be exploited to suppress the background further, but the required two orders of magnitude are presumably very hard to obtain. Thus, the channel $N \to e^- + 2$ jets is not useful for a search strategy. As noted earlier, the family mixing decay $N \to \mu^- W^+$ would not suffer from this problem but should be observable similar to the positron signal.

The decay $N \to \nu + Z$ with $Z \to q\bar{q}$ gives the signal of missing $p_\perp$ plus two jets. For the Majorana neutrino masses reachable at HERA the branching ratio into light neutrinos is rather small (Fig. 2), making this signal less attractive. The main problem at both HERA and LEP⊕LHC is, however, the background from charged current DIS which is overwhelming even after jet requirements as shown in Fig. 7ef.

4.4.2 Two high-$p_\perp$ leptons

For the signal based on the leptonic decay of the W/Z, we require a second isolated high-$p_\perp$ charged lepton with opposite charge compared to the first one and having $p_\perp > 10$ GeV and $-1 < y_\ell < 3$ for $m_N = 100$ GeV at HERA and $p_\perp > 20$ GeV and $0 < y_\ell < 3$ for $m_N = 500$ GeV at LEP⊕LHC. The isolation of this second lepton is demonstrated in Fig. 8, which shows the variation of the cross section with the allowed accompanying energy within a cone $\Delta R = 0.5$. The distribution is very flat allowing a stringent cut, which is here chosen as $E_{acc} < 1$ GeV. These cuts also reduce the backgrounds far below the signal as seen in Fig. 8 and demonstrated step by step in Table 3.

The theoretically available cross section at LEP⊕LHC is $86\ fb \times 67\% \times 21\% = 12\ fb$ for $N \to e^\pm W^\mp$, $W \to \ell\nu_\ell$ and $86\ fb \times 33\% \times 7\% = 2\ fb$ for $N \to \nu Z$, $Z \to \ell^+\ell^-$ ($\ell = \mu$ or e). The small branching ratio for the latter decay chain implies that the invariant mass of the lepton pair will usually not be a useful quantity, explaining the low cross-section in Table 3 obtained when requiring this quantity to be around the Z mass. The total cross-section for the two-lepton case is thus $14\,fb$ to be compared with the extracted $11\,fb$ ($20\,fb$ and $14\,fb$, respectively, at HERA), which demonstrates the efficiency of our search strategy.

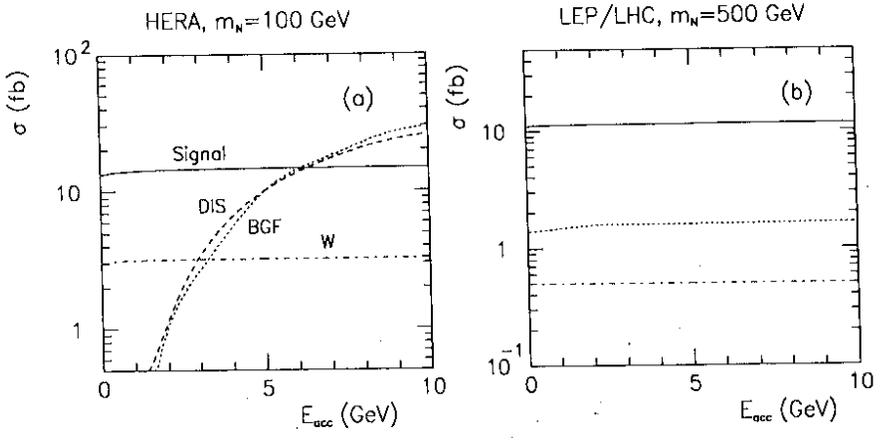

Figure 8: *Isolation test as in Fig. 6, but for the second highest $p_\perp$ lepton in the event sample given by the two-lepton signature, where the first lepton is of opposite charge and fulfills the requirements on $p_\perp$, rapidity and isolation.*

	Applied cut	Signal	DIS	BGF	W
HERA	Lepton 1: $p_\perp > 10$, $-1 < y_\ell < 3$, $E_{acc} < 1$	60	681908	4204	105
($m_N = 100$)	Lepton 2: $p_\perp > 10$, $-1 < y_\ell < 3$, $E_{acc} < 1$	14	0.	0.	3.2
	$86 < m_{\ell_i \ell_j} < 96$	0.57	0.	0.	0.
LEP⊕LHC	Lepton 1: $p_\perp > 100$, $0 < y_\ell < 3$, $E_{acc} < 1$	67	26228	249	54
($m_N = 500$)	Lepton 2: $p_\perp > 20$, $0 < y_\ell < 3$, $E_{acc} < 1$	11	0.	1.6	0.5
	$86 < m_{\ell_i \ell_j} < 96$	1.1	0.	0.01	0.

Table 3: *Cross-sections [fb] for two isolated high $p_\perp$ leptons.*

4.5 Majorana neutrino mass reconstruction

The mass of the Majorana neutrino can be reconstructed from the four-momenta of the positron and the two reconstructed jets as shown in Fig. 9ab, resulting in a very clear and narrow peak around $m_N = 100\ GeV$ and $m_N = 500\ GeV$, respectively. Given the background free situation, this should provide a measurement of the Majorana neutrino mass even with low statistics. The width of the heavy Majorana neutrinos is $2\ MeV$ for $m_N = 100\,GeV$ and $400\ MeV$ for $m_N = 500\,GeV$, but in the simulation there is no event-to-event variation of the neutrino mass since this very narrow width is well approximated by a delta function.

In case of the two-lepton signal it is more difficult to reconstruct the Majorana neutrino mass due to the presence of a neutrino which escapes detection. The invariant mass of the two isolated leptons and the $\not{p}_\perp$-vector, representing the neutrino from the W decay (and only rarely from the $N \to \nu Z$ decay), gives the mass distributions in Fig. 9cd that are poor estimates of the Majorana neutrino mass. Instead of simply neglecting the longitudinal momentum of the decay neutrino, this mass reconstruction can be improved by using the value of $p_{\nu\parallel}$ which together with one of the leptons give the invariant mass of the W. The

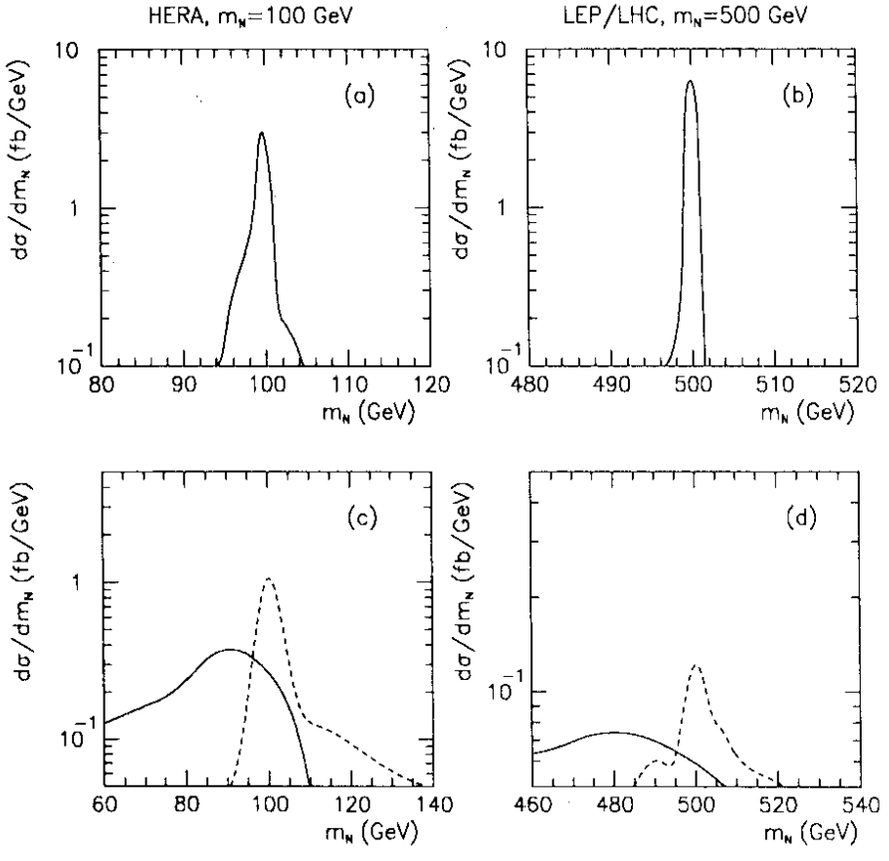

Figure 9: *Reconstruction of the Majorana neutrino mass through the invariant mass based on (a,b) the isolated positron and the two jets (which reproduce the W-mass within ±5 GeV) and (c,d) the two isolated leptons and the neutrino represented by $\not{p}_\perp$ alone (full curves) and using also the $p_{\nu\parallel}$-value which reproduce the W mass (dashed curves). (a,c) HERA with Majorana neutrino mass $m_N = 100\ GeV$, (b,d) LEP⊕LHC with $m_N = 500\ GeV$.*

problem is to assign the right lepton to the W-decay. With $m_N = 100\ GeV$ at HERA, the largest energy release is in the W decay which therefore gives the lepton with highest $p_\perp$, whereas with $m_N = 500\ GeV$ at LEP⊕LHC one should select the second highest $p_\perp$ lepton with opposite charge to the first one. Using this assignment we obtain the peaks shown in Fig. 9c and d, respectively. Since the background is quite small also for this signal (cf. Table 3), the Majorana neutrino mass should be measurable with a few events also in this case. However, the absolute cross-section in the peak at LEP⊕LHC is for this signal too small to make it useful in any mass-determination.

	Mass	y_ℓ^{min}	y_ℓ^{max}	$p_{\perp min}^{positron}$	$p_{\perp min}^{lepton1}$	$\not{p}_{\perp min}$	$p_{\perp min}^{lepton2}$
HERA	$m_N = 100$	-1	3	10.	10.	10.	10.
	$m_N = 160$	-1	3	10.	10.	10.	10.
LEP⊕LHC	$m_N = 100$	-1	1	10.	10.	10.	10.
	$m_N = 300$	0	3	50.	50.	50.	20.
	$m_N = 500$	0	3	100.	100.	100.	20.
	$m_N = 700$	0	3	150.	150.	150.	50.

Table 4: *Cuts used in search for Majorana neutrinos of different masses.*

5 Summary and conclusions

We have discussed extended gauge theories, e.g. with the electroweak symmetry group $SU(2)_L \otimes U(1)_Y \otimes U(1)_{Y'}$, which predicts the existence of heavy Majorana neutrinos N. The production in ep collisions proceeds via W exchange and is suppressed by a small mixing $|(V\xi)_{eN}|^2$. The dominant decays are $N \to e^\pm W^\mp$ and $N \to \nu_e Z$, where the lepton number can be violated, followed by the subsequent decays $W^\pm \to \ell^\pm \nu_\ell$, $W^\pm \to q\bar{q}'$ and $Z \to \ell\ell$, $Z \to q\bar{q}$. Present experimental information have been examined with respect to the resulting bounds on mass and mixing of these Majorana neutrinos, with the conclusion that masses as low as $100 GeV$ and mixings as large as 1% are not excluded. As a result the production cross-sections at the HERA and LEP⊕LHC ep colliders can be large enough to be experimentally accessible and give observable signals in terms of high-$p_\perp$ leptons and jets.

In order to study the phenomenological aspects of production and decay of heavy Majorana neutrinos in more detail, we have constructed a dedicated Monte Carlo program which simulates complete events. The dominant background processes are deep inelastic scattering, heavy flavor production and W boson production; all of which have been Monte Carlo simulated in order to find realistic search strategies for Majorana neutrinos at ep colliders. The DIS background overwhelms the signal based on the final states $e^- W^+ (\to q\bar{q}')$ and $\nu_e Z (\to q\bar{q})$ from heavy neutrino decays. Hence, one has only useful signals based on the final states $e^+ W^- (\to q\bar{q}')$ and $e^\pm W^\mp (\to \ell^\mp \bar{\nu})$. With the non-diagonal elements in the mixing matrix $V\xi$ different from zero, the resulting decays $N \to \mu^\pm W^\mp$ would both be experimentally very useful due to the usually efficient muon detection whereas the decays $N \to \tau^\pm W^\mp$ would be more difficult to use. For these 'useful' decay modes all backgrounds can be eliminated by means of an appropriate isolation requirement on high-$p_\perp$ leptons, combined with W mass reconstruction from jets in the case of hadronic W decays. It is furthermore possible to reconstruct the Majorana neutrino mass from its measured decay products. The essentially 'background-free' events, such as the decay $N \to \nu Z$, with $Z \to \mu^+\mu^-$ and large missing transverse momentum have too small branching ratios to give any contribution at HERA and at LEP⊕LHC the uncertainty in the missing transverse momentum is too large to make it useful for a Majorana mass reconstruction.

Our detailed Monte Carlo simulation results presented above are case studies for selected neutrino masses and mixing. To give a more complete picture of the prospects for exploring the Majorana neutrino scenario we have also investigated some other masses with the main results shown in Table 5 and 6. The larger the neutrino mass, the larger transverse momenta of its decay products and we have therefore modified the cuts according to Table 4.

	Mass	Signal	DIS	BGF	W	min ξ^2
HERA	$m_N = 100$	9.4	0.	0.	.1	0.006
	$m_N = 160$	2.0	0.	0.	.1	0.02
LEP⊕LHC	$m_N = 100$	91	0.	4.1	5.6	0.001
	$m_N = 300$	43	0.	1.6	2.9	0.001
	$m_N = 500$	13	0.	0.2	0.9	0.004
	$m_N = 700$	2.3	0.	0.01	0.2	0.02

Table 5: *Cross-sections [fb] and ξ^2-limits for Majorana neutrino search based on positron and reconstructed W-mass.*

	Mass	Signal	DIS	BGF	W	min ξ^2
HERA	$m_N = 100$	14	0.	0.	3.2	0.004
	$m_N = 160$	2.7	0.	0.	3.2	0.02
LEP⊕LHC	$m_N = 100$	103	0.	0.8	22	0.002
	$m_N = 300$	38	0.	3.0	2.1	0.001
	$m_N = 500$	11	0.	1.6	0.5	0.005
	$m_N = 700$	1.7	0.	0.04	0.	0.03

Table 6: *Cross-sections [fb] and ξ^2-limits for Majorana neutrino search based on two isolated high $p_\perp$ leptons.*

The mixing parameter ξ, which is a free parameter, enters only as an overall factor and it is therefore straightforward to estimate its lower limit where the cross-section becomes too low for experimental observation. From the relevant cross-sections (after all cuts) in Table 5 and 6 one obtains the ξ^2-limits given, by requiring the signal cross-section to be at least as large as the background level and, in addition, to be large enough to produce a minimum of five events for an integrated luminosity of 1 fb^{-1}. Thus, one can conclude, from the cross-sections for a high-$p_\perp$ positron and two jets, that it should be possible to discover a Majorana neutrino at HERA provided that, e.g., its mass is around 100 GeV and its mixing not smaller than 0.6%, whereas at LEP⊕LHC the corresponding discovery limit is 500 GeV if the mixing is at least 0.4%. If one adds the two signals in Table 5 and 6 and requires five events, then the discovery limits are increased to about 700 GeV at LEP⊕LHC and 160 GeV at HERA for a mixing of 1%. If no events are found, the limits on the mass and mixing of Majorana neutrinos should be correspondingly improved.

Acknowledgement: We are grateful to M.B. Voloshin for a valuable discussion on Majorana neutrino mass limits, and to W. Buchmüller and C. Greub for helpful discussions and advice as well as to F. Kole for assistance with the W background generator. This work was supported in part by the Swedish Natural Science Research Council.

References

[1] R.N. Mohapatra, P.B. Pal, 'Massive neutrinos in physics and astrophysics', World Scientific 1991
'Neutrinos', Ed. H.V. Klapdor, Springer Verlag 1988

[2] W. Buchmüller, C. Greub, Nucl. Phys. B363 (1991) 345

[3] W. Buchmüller, C. Greub, P. Minkowski, Nucl. Phys. B381 (1992) 109

[4] W. Buchmüller, C. Greub, Nucl. Phys. B381 (1992) 109

[5] W. Buchmüller et al., in proceedings 'Physics at HERA', Eds. W. Buchmüller, G. Ingelman, DESY Hamburg 1992, vol. 2, p. 1003

[6] W. Buchmüller, C. Greub, Phys Lett. B256 (1991) 465

[7] D. Duke, J.F. Owens, Phys. Rev. D30 (1984) 49

[8] M.Z. Akrawy et al., OPAL collaboration, Phys. Lett. B247 (1990) 448

[9] O. Adriani et al., L3 collaboration, Phys. Lett. B295 (1992) 371

[10] Review of particle properties, Phys. Rev. D45 (1992)

[11] K. Muto, E. Bender, H.V. Klapdor, Z. Phys. A 334 (1989) 187

[12] F. Simkovic et al., Z. Phys A 341 (1992) 193

[13] P. Langacker, D. London, Phys. Rev. D38 (1988) 886

[14] W. Buchmüller, C. Greub, H.-G. Kohrs, Nucl. Phys. B370 (1992) 3

[15] J. Rathsman, G. Ingelman, MAJOR 1.1, in proceedings 'Physics at HERA', Eds. W. Buchmüller, G. Ingelman, DESY Hamburg 1992, vol. 3, p. 1513

[16] J. Rathsman, Diploma thesis, Uppsala preprint TSL/ISV 92-0058

[17] E. Eichten, I. Hinchliffe, K. Lane, C. Quigg, Rev. Mod. Phys. 56 (1984) 579, ibid. 58 (1986) 1047

[18] G. Ingelman, LEPTO 6.1, in proceedings 'Physics at HERA', Eds. W. Buchmüller, G. Ingelman, DESY Hamburg 1992, vol. 3, p. 1366

[19] T. Sjöstrand, JETSET 7.3, CERN-TH.6488/92

[20] B. Andersson, G. Gustafson, G. Ingelman, T. Sjöstrand, Phys. Rep. 97 (1983) 31

[21] G. Ingelman, G. A. Schuler, AROMA 1.4, in proceedings 'Physics at HERA', Eds. W. Buchmüller, G. Ingelman, DESY Hamburg 1992, vol. 3, p. 1346

[22] U. Baur, J.A.M. Vermaseren, D. Zeppenfeld, Madison preprint MAD/PH/675

[23] E. Theuer, 'Monte Carlo Untersuchungen der W-boson Produktion und konkurierender Prozesse bei HERA', Diplomarbeit, Technische Hochschule Aachen

[24] M. Fleischer et al., in proceedings 'Physics at HERA', Eds. W. Buchmüller, G. Ingelman, DESY Hamburg 1992, vol. 1, p. 303

[25] V. Hedberg et al., in proceedings 'Physics at HERA', Eds. W. Buchmüller, G. Ingelman, DESY Hamburg 1992, vol. 1, p. 331